Calculating the Segmented Helix Formed by Repetitions of Identical Subunits and a Zoo of Platonic Helices

Robert L. Read *email read.robert@gmail.com

Founder, Public Invention, a non-profit.

August 24, 2019

Abstract

Eric Lord has observed:

> In nature, helical structures arise when identical structural subunits combine sequentially, the orientational and translational relation between each unit and its predecessor remaining constant.[1]

This paper proves Lord's observation as a consequence of screw theory. Constant-time algorithms are given for the segmented helix generated from the intrinsic properties of a stacked object and its conjoining rule. Standard results from screw theory[2] and previous work for finding the axis of a helix from points[3] are combined with corollaries of Lord's observation to allow calculations of segmented helices from either transformation matrices or four known consecutive points. The construction of these from the intrinsic properties of the rule for conjoining repeated subunits of arbitrary shape is provided, allowing the complete parameters describing the unique segmented helix generated by arbitrary stackings to be easily calculated. Free-libre open-source interactive software[4] is provided which performs this computation for arbitrary prisms along with 3D visualization[5]. This allows the deduction of intrinsic properties of a repeated subunit from known properties of a segmented helix, as a chemist might want to do. Because the algorithms are efficient, a repeated subunit can be designed to create a segmented helix of desired properties, as a mechanical engineer or robotocist might want. A proof is provided that any subunit can produce a toroid-like helix or a maximally extended helix, forming a continuous spectrum based on joint-face normal twist. As a verification and demonstration, the software and paper compute, render, and catalog an exhaustive "zoo" of 28 uniquely-shaped platonic helices, such as Boerdijk-Coxeter tetrahelix and various species of helices formed from dodecahedra, for example.

*read.robert@gmail.com

Contents

1 Introduction

During the Public Invention Mathathon of 2018[6], software was created to view chains of regular tetrahedra joined face-to-face. The participants noticed that whenever the rules for which face to add the next tetrahedron to were periodic, the resulting structure was always like a discrete helix.

Although unknown to us at that time, we now call Lord's Observation:

> In nature, helical structures arise when identical structural subunits combine sequentially, the orientational and translational relation between each unit and its predecessor remaining constant.[1]

The purpose of this paper is to prove Lord's Observation and provide mathematical tools and software for studying arbitrary segmented helices generated in this way.

Finding the properties of a segmented helix from three contiguous segments on the helix from screw theory[7, 2, 8, 3], is explained and formulated. An interactive, 3D rendering website written in JavaScript which allows both calculation and interactive play and study[5]. This allows a structure or molecule coincident to a segmented helix to be designed by adjustments to the repeated object, or for the shape of a repeated subunit to be inferred from the intrinsic properties of the segmented helix. Kahn's method [3] is modified to cover some degenerate situations.

We exploit Lord's Observation to discover symmetry which allows us to compute the helix when subunits are joined face-to-face with the same *twist*. Kahn was investigating proteins, which do not have faces, but geometric solids and other macroscopic solid objects do. This concept can be generalized to a *joint face angle*, even if the objects conjoined do not technically have flat faces. This symmetry allows us compute the parameters of the segmented helix purely from properties intrinsic to a single object and the joining rule. We prove that vaarying the *twist* of the joint faces through a complete rotation produces a smoothly varying spectrum of shapes that always includes a torus-like shape and a "zig-zag" planar segmented helix of maximal extent Finally, as an important demonstration, these tools are used to produce a catalog of all possible helices generated by vertex-matched face-to-face joints of the Platonic solids, of which only the tetrahelix[9, 10, 11, 12, 13] has been completely described to date.

2 A Warm-up: Two Dimensions

Considering the problem in two dimensions may be a valuable introduction. Suppose that we consider a polygon that that as two edges, called A and B, and that we define the length L of the polygon as the distance between the midpoints of these edges. Suppose that we are only allowed to join these polygons by aligning A of one polygon to B of another polygon, with their midpoints coincident. Let us further assume that we disallow inversions of the polygon. Let us imagine that we have a countable number of polygons P_i indexed from 0. Then what shapes can we make by chaining these polygons together?

Each joint J_i between polygons P_i and P_{i+1} will place the axes of the polygons at the same angle, θ, since our polygons do not change shape. Let us define θ to be

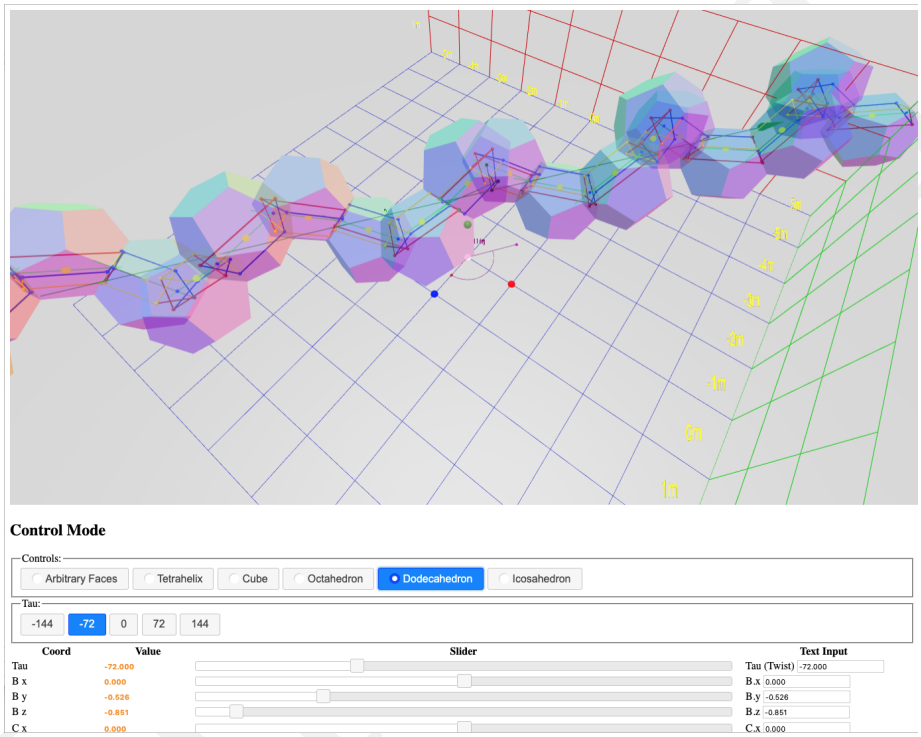

Figure 1: Example Segmented Helix Generated From the Dodecahedron

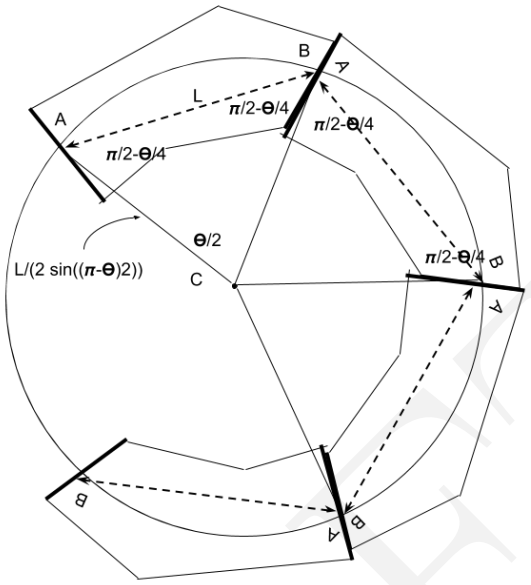

Figure 2: A 2D Analog of a Helix Generated by Repeated Subunits

positive if we move anti-clockwise from P_i to P_{i+1} and negative if we move clockwise. If $\theta = 0$, the joints will be collinear.

If $\theta \neq 0$, the polygon joints will always lie on a circle. A proof of this is that each polygon has associated with it an isosceles triangle A, B, C, where $\angle CBA = \angle CAB = \theta/2$, and $\angle ACB = (\pi - \theta)$. AC and BC are not necessarily aligned with an edge of the polygon. The length AB is L, and the lengths AC and BC are $(L/2)/\sin(\pi - \theta)/2$. In any chain of polygons, these triangles all meet at point C, and there all joints are on the circle centered at C with radius $\frac{L}{2\sin\frac{\theta}{2}}$.

3 The Segmented Helix

An analogous result holds in three dimensions.

In this section we consider a helix evaluated only at regular points.

Following the Wikipedia article `https://en.wikipedia.org/wiki/Helix`, we set up a helix parametrically.

$$P_x(t) = r\sin t$$
$$P_y(t) = r\cos t$$
$$P_z(t) = bt$$

Such a helix has a radius of r and slope (if $r \neq 0$) of b/r. The pitch of helix, the change in t needed to make one complete revolution, is $2\pi b$. Note that a helix may be degenerate in two ways. If $r = 0$, these equations become a line. If $b = 0$, these equations describe a circle in the xy-plane. If $r = 0$ and $b = 0$, the figure is a point.

Such helices are continuous, but we are investigating stacks of discrete objects. We in fact wish to derive the parameters for a continuous helix from such discrete objects which constrain discrete points, so we wish to study a helix evaluated at integral points. Call such an object a *segmented helix*. A segmented helix may be thought of as function that given an integer gives back a point in three space.

$$P_x(n) = r \sin n\theta$$
$$P_y(n) = r \cos n\theta$$
$$P_z(n) = nd$$

d is the distance or *travel* along the axis between adjacent joints. In this canonical representation this is the z-axis. θ is the rotation around the z-axis between adjacent points. r is the radius of the segmented helix. Note that if $\theta = \pi$, we have a third form of degeneracy (to the human eye) of a segmented helix which is a zig-zag contained completely within a single plane.

If we think of the segmented helix as describing a polyline in 3-space, we would like to investigate the properties of that polyline. If we consider only the intrinsic shape of the segmented helix, there are three degrees of freedom: r, d, θ. We call these the *intrinsic* properties of the segmented helix.

Figure 3 demonstrates our conventional concepts. It is a screen shot taken from our interactive software[5]. The software allows parallax by supporting interactive rotation, which makes the 3D structure easier to understand; we encourage the reader to visit our interactive page as we discuss our naming conventions.

In Figure 3 and our software, we represent the object as a prism with triangular cross-section, because this is the simplest physically realizable macroscopic object that supports a face-to-face connection. In this diagram, the points A, B, C, D are represented by the sphere of the same color as the label. The view is roughly in the direction of the axis of the segmented helix, which is drawn as a dark green arrow, pointing in the positive z and positive x direction, parallel to the XZ-plane. For ease of viewing, the entire segmented helix has been raised by two units on the y axis. The segment $\overline{BC}$ has coordinate $y = 2$, and is aligned with the z-axis, and centered in z direction.

The positive axes x, y and z axes are shown by the red, green and blue axes, respectively. Following computer graphics convention, the y axis is oriented vertically. The points A, B, C, D correspond to $P(0), P(1), P(2)$, and $P(3)$ for a segmented helix aligned to this axis (not the z-axis.) A thin green polyline represents the segmented helix, and thus connects the joints A, B, C, and D. The points are wrapping around the axis clockwise, with an angle of $\theta = 56.6°$ as show by the on-screen protractor as the rotation from one point to the next. As will be explained in Section 8, τ is the face-on-face joint rotation of 45°. The helix angle $\phi = 39.7°$ is rendered by a protractor on the $y = 0$ plane; this the angle between the axis and of the helix and the z axis, and therefore the angle of any one segment against the helix angle.

A line is drawn from the blue point B to an black sphere on the helix axis. The

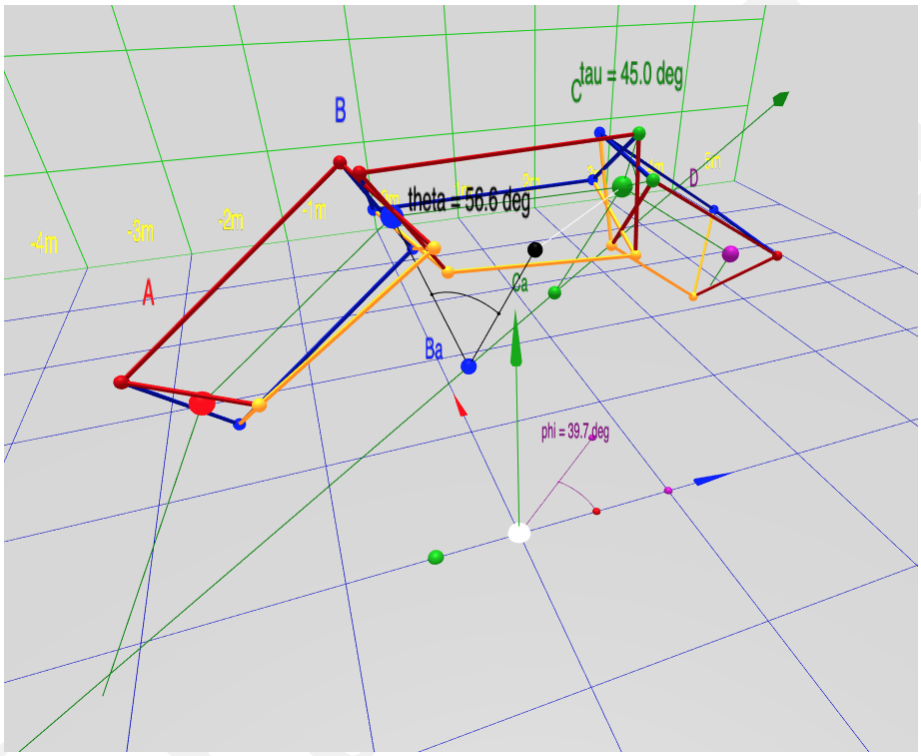

Figure 3: Naming of measures

point on the helix axis, which renders it as a black sphere, is denoted B_a. Analogously, C_a is the point on the axis closest to he green point C.

A segmented helix located in space is completely determined by these parameters, a vector describing the axis of the helix, and the position of any one joint.

Because the segmented helix is a discrete structure, we reframe the concept of *pitch* as *sidedness* s: how many segments (sides) make a complete rotation?

The following concepts and conventional variable names for them will be related:

- L is the distance between any two adjacent points (that is, between B and C, for example.)
- r is the distance between a point and the helix axis (that is, B and B_a for example.)
- θ is the rotation about the axis between two consecutive joints about the helix axis.
- c is the length of a chord formed by the projection of the segment between two points projected along the axis of the segmented helix (A chemist may recognized this as the distance betwen residues on a *helical wheel* projection).
- d is the distance along the axis of the helix between any two joints (B_a and C_a, for example, rendered as a small black and blue sphere, respectively in Figure 3.
- ϕ is the angle between any vector between two adjacent joints and the axis of the helix. In physical screws used in mechanical engineering, this is analogous to the *helix angle* [14].
- p is the pitch of the helix, the distance traveled in one complete rotation.
- s is the number of segments in a complete rotation (in general not rational.)
- Finally, we find it useful to define the *tightness* of a segmented helix as travel divided by radius, a number analogous to the extension of a coil spring or slinky. A torus-like segmented helix has zero tightness and a zig-zag has maximum tightness. The symbol t represents tightness.

These quantities are related:

$$c = 2r \sin \frac{\theta}{2} \tag{1}$$

$$L^2 = c^2 + d^2 \tag{2}$$

$$\arctan \frac{c}{d} = \phi \tag{3}$$

$$s = \frac{2\pi}{\theta} \tag{4}$$

$$d = L \cos \phi \tag{5}$$

$$p = ds \tag{6}$$

$$t = d/r \tag{7}$$

$$\tag{8}$$

Measuring ϕ requires us to decide on the sign of the direction of the axis, which is arbitrary and not based on the physical shape.

Any point on on the segmented helix has a closest point on the axis of the helix. In particular, we will call the points closest to the joints *joint axis points*. Then d is the distance along the axis between consecutive joint axis points.

We seek to relate these properties to properties intrinsic to the joint or interface between two segments or objects in the segmented helix. If given an object, the length L between the joints L.

3.1 Sign Conventions for Spatially Located Segmented Helices

When thinking about the overall shape of a segmented helix, one is likely to be interested in the absolute magnitude of its intrinsic properties.

However, when doing doing computer graphics work or kinematic calculations, the sign conventions are critical. Because this paper wishes to emphasize the continuum of shapes produced by changing an object used to generate the segmented helix, and in particular is interested in the degenerate helix which produces toroidal figures, we prefer to be able to discuss the axis of a segmented helix as a existing even when the figure has no travel along the axis (that is, when $d = 0$).

Therefore we elect the following conventions:

- A right-handed coordinate system.
- The helix axis is a normalized vector which never vanishes.
- The travel along the axis (d) is negative when the helix is counterclockwise (that is, when motion from joint n to joint $n+1$ appears counterclockwise when $\theta < \pi$, zero when toroidal, and positive when the helix is clockwise.
- θ is never negative.

4 The Intrinsic Properties of Periodic Chains of Solids

If we have chains of identical repeated 3D units conjoined identically, or *periodic chains*, they generate a segmented helix coincident on their joints. Although fairly obvious from Chasles' Theorem, we have not found this stated in writing elsewhere, so we call this Lord's Observation:

Observation 1 (Lord's Observation)**.** *In nature, helical structures arise when identical structural subunits combine sequentially, the orientational and translational relation between each unit and its predecessor remaining constant.[1]*

Lord's Observation may perhaps be clarified that in fact identical objects conjoined via a rule produce periodic chains of objects that are uniformly intersected by segmented helices and that they may be degenerate in one of three ways that we might not strike the human eye as a helix if we are not seeking them:

1. The segments may form a straight line. (For example, see Figure 11).
2. The segments may be planar about a center, forming a polygon or ring. (For example, see Figure 17).
3. The segments may form a planar saw-tooth or zig-zag pattern of indefinite extent (For example, see Figure 4).

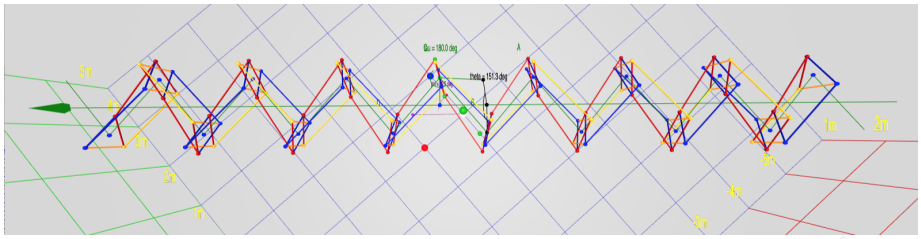

Figure 4: A Planar Zig-Zag

There are two complementary ways of learning about such segmented helices. In one approach, we may have knowledge of the segmented helix, and wish to learn about the subunits and the rule with which the subunits are combined. For example, we may have microscopic objects such as proteins or atoms, and we know from crystallography something about the positioning of these objects, without knowing ahead of time the angles at which these objects would combine in their natural environment. In this case, we use a variant of a linear algebra method[3] for determining the radius, travel, and twist of the segmented helix (these terms will be defined precisely below.)

In the other approach, we may know *a priori* exactly the relevant properties of the objects and the rule which which they combine, and we seek to compactly describe the segmented helix they create. For example, a mathematician may consider a chain of dodecahedra, or a woodworker may cut identical blocks of maple wood, which are to be glued together face-to-face. In these cases everything about the objects and the rules for conjoining is known before the first two objects are glued together. We call this the *joint face normal method*, because it can be simulated by joining two flat faces together with a specified twist, even if the objects in question do not actually have a physical face (such as molecules).

In both cases, we would like to understand how a change in a face normal or a twist affects the parameters of the segmented helix, and, conversely, we would like to be able to choose the construction of the subunits to achieve a particular segmented helix.

In engineering, sometimes the term *special helix*[15] is use for helical curves on non-cylindrical surfaces. This paper use the term *helix* only in the sense of *cylindrical helix*.

5 Periodic Chains Produce Segmented Helices

A periodic chain is in fact a simple object which demonstrates tremendous symmetry. Before using this symmetry in the construction of the segmented helix corresponding to a periodic chain, we prove that such a segmented helix indeed exists for every periodic chain.

Theorem 1 (Segmented Helix)**.** *Consider N identical objects which each have two points, A and B, called* joints*. Call $\overrightarrow{AB}$ the* axis *of this object. Consider the frame of reference for this object to have its axis on the z-axis with B in the positive direction, the midpoint of the object at the origin.*

Consider any rule that conjoins A of object $i+1$ to B such that from the frame of reference of i, the object $i+1$ and anything rigidly attached to it is always in the same position in the frame of reference for i. Informally, $i+1$ "looks the same" to i, no matter what i we choose, $i < N$. Call a chain of N identical rigid objects conjoined via a rule that conjoins A_i to B_{i+1} in such a way that every vector of B is always in the same position relative to a frame of reference constructed from A a periodic chain.

Any periodic chain of three or more objects has a unique segmented helix who whose segments correspond to the axes of these objects.

Proof. We will proceed by induction.

Base Case ($k == 3$):

Take an object AB. By Chasles' theorem[16] there is a screw axis S, a set of rotations, and a transposition d which moves the first object to position where the second object BC is. Take one of the rotation angles of smallest value. Construct the points A', B' and C' as the closest points to A, B and C on this axis. These points are collinear by construction.

Now add the object CD to object BC by our the rule of periodic chains. Consider the points B' and C' from A's frame of reference. Let $d = \|\overline{C}' - \overline{B}'\|$. Construct the point D' on our screw axis as the point closest to D on that line.

Now because $C'D'$ in BC's frame or reference must look like $B'C'$ in A's frame of reference, the distance $\|\overline{D}' - \overline{C}'\| = d$. From A's frame of reference, $A'B'C'$ are collinear, so the points $B'C'D'$ must be collinear in B's frame of reference.

In any frame of reference, if $A'B'C'$ are collinear and $B'C'D'$ are collinear, then $A'B'C'D'$ are collinear.

Now, looking backward from CD towards A, the distance $A'B'$ must be the same as the distance $B'C'$ so as to not violate our rule. So $d = \|A'B'\| = \|B'C'\| = \|C'D'\|$. Similarly because by construction $r = \|BB'\| = \|CC'\|$, and AA' is a rigid transformation of BB', so $r = \|AA'\|$. By symmetry, $r = \|DD'\|$. Compute θ as the rotation about S that takes BB' into CC'. By our rule of attachment, θ also takes CC' into DD' and AA' into BB'.

Now construct a segmented helix, the radius r, distance, and angle θ. This segmented helix can be positioned coincident with S so that $H_0 = A$. Then $H_1 = B$, $H_2 = C$, and $H_3 = D$.

Therefore, for the base case of three objects, there is a segmented helix whose segments coincide with the axes of the objects.

Inductive Case ($k+1$): Assume there is a segmented helix coinciding with the first k objects, and consider the frame of reference of the kth object. The axis and any other rigid property of the $k+1$th object stands in relation to object k as k stood to $k-1$. By induction, the kth object had a segment of a segmented helix corresponding to its axis. Attach vectors V_{Ak} and V_{Bk} from the joints of k to the axis of the helix perpendicularly. Define these vectors in the frame of reference for k.

To the $k-1$th, the tips of V_{Ak} and V_{Bk} define a line segment which lies on the axis of the segmented helix H, with the tip of V_{Ak} coincident with the tip of $V_{B(k-1)}$.

By our rule and by induction, since this is true of the $k-1$th object, it is true of the kth object. Therefore the $k+1$th objects V vectors V_{Ak+1} and V_{Bk+1} point to a

line segment which lies on the axis of H, extending it in the same direction. The axis of the $k+1$th object therefore coincides with the $k+1$th segment of H.

Therefore, by induction, identical objects conjoined by the same rule always coincide with some segmented helix, whose parameters are discoverable. □

In engineering the term *helix angle* refers to the angle between a line tangent to a continuous helix and the axis of the helix. In segmented helices, this is the same as the angle between the axis of each object in a periodic chain and the axis of the segmented helix coincident to it.

It is perhaps not obvious when one considers objects which are, taken as individuals, highly asymmetric, that the helix angle of the segmented helices produced by by periodic chains are the same for each object. For example, The B face does not have to be the same size as the A face. In fact, the object itself might be shaped like the letter "C", and not completely enclose the axis. Taking the idea further, the object might be spiky like a stellated polyhedron or a sea urchin, and still be joined by joints relatively close to the center of the object. In this paper we do not concern ourself with the issue of self-collision of the objects, which would have to be considered if one attempted to make a period chain of sea urchins.

Corollary 1 (Segment Similarity)**.** *The helix angle of any object axis in a periodic chain is the same.*

Proof. The axes of each object coincide with a segment of a segmented helix. A segmented helix is completely symmetric no matter in which direction of the axis you look down or which point on the axis you begin at. The angle between each pair of objects is exactly the same. □

Corollary 1 will be used in our development of *PointAxis* algorithm and in our computation of segmented helix properties and to justify balancing face normals to produce an intrinsic out-vector and to apply the *PointAxis* algorithm without actually assigning objects Cartesian coordinates.

6 Computing Screws and Segmented Helices from Transformation Matrices

The rule for how objects in a periodic chain are joined may be conveniently captured as a transformation matrix. In general, a human engineer will have to compute this transformation matrix from some other information, such as the face-to-face conjoining rule. We discuss how to do this from joint-face normal vectors in Section 8. However, a transformation matrix clearly capture the idea of "repetition". Since by definition the objects in the chain are the same shape, moving one object into a new position and place an identical copy of that object in that position are practically the same.

Using standard screw theory[2, 8], a screw can be computed from such a transformation matrix. This consists of the axis of the screw S, a point on the screw axis P, the rotation θ around the axis, and the transposition, or travel, along the axis of one transformation.

Neither a transformation matrix or its corresponding screw completely define all of the intrinsic properties of a segmented helix. In particular, a matrix M maps any point p to a point p'. Since this applies to all points no matter how far from the screw axis or the axis of rotation and such transformation preserve distance to this axis (the radius), the radius of a segmented helix is not determined by a transformation matrix or a screw. Since the helix angle ϕ changes with radius for a helix of a given pitch, ϕ is not determined.

However, if we have a screw and one point on the axis of the screw fixing it in space and the location of one joint, all of the properties of the segmented helix are completely determined.

In our software, we have coded the calculation of the screw directly from a transformation matrix, and the additional routines which determine all intrinsic properties from a joint position (making certain arbitrary alignment choices without loss of generality.)

Although not original to this paper, the author found it difficult to find clear documentation on how to calculate the screw from the transformation matrix. We therefore include an exposition here, in hope it will be useful, and a valuable adjunct to the code to a programmer seeking to duplicate this functionality.

6.1 Computing the Screw Axis from a Transformation Matrix

Our goal is to compute a normalized vector $\hat{H}$ aligned with the screw axis of the transformation effected by a transformation matrix R.

In order to be robust, it is valuable to check that the transformation matrix is a rigid transformation[17], as Chasles' theorem applies only to rigid transformations. Transformation matrices in homogeneous coordinates, as typically used in kinematics and computer graphics, are convenient for this purpose, allow a the transformation represented by a matrix to be effected by simple multiplication.

The angle of rotation is computable from the trace of R, $Tr(R)$.

$$\theta = \arccos \frac{Tr(R) - 1}{2} \tag{9}$$

Technically, arccos is multi-valued, but we will take θ to be in its principle range, $0 \leq \theta \leq \pi$. If θ is 0 or a multiple of π, then we the *zig-zag* degenerate case, the method of compute H from the rotation basis of R is numerically unstable. However, in this case we can compute the direction vector H as the difference vector between an arbitrary point q (a 4x1 vector in homogeneous coordinates) and its transformation performed twice. Informally, this is a "zig, then a zag".

$$H = R(R(q)) - q \tag{10}$$

(Note that in general H is not normalized, $H \neq \hat{H}$. Also recall that multiplication by a transformation matrix produces a point that in a new position representing the transformation.)

In other cases, H can be computed from the direction cosines of R[18]:

$$R = \begin{bmatrix} a & b & c' & x \\ d' & e & f & y \\ g & h & i & z \\ 0 & 0 & 0 & 1 \end{bmatrix} \tag{11}$$

$$H = \begin{bmatrix} h - f \\ c' - g \\ d' - b \\ 1 \end{bmatrix} \tag{12}$$

(The variables c' and d' are marked to distinguish them from the symbols for the chord c and the travel along the axis d.) The magnitude of $\|H\| = 2\sin\theta$, which vanishes when θ is 0 or multiple of π, hence our need to treat those cases differently.

Although the matrix R in general produces both a rotation and a translation in space, distance between q and Rq in general depends on how far q is from the axis of rotation. However, the travel d along the axis of the rotation does not depend on q. It can be computed as a dot product:

$$d = \overrightarrow{BC} \cdot \hat{H} \tag{13}$$

These are the only properties that can be computed from the matrix R alone; but once we have the length along the object axis (*not* the helix axis) L of an object we can compute our computations, based on relations already given in Section 3.

The chord of the segmented helix (that is, length of an object of axis length L projected along H) is:

$$c = \sqrt{L^2 - d^2} \tag{14}$$

Knowing the chord c and the amount of rotation θ allows us to compute the radius:

$$r = \frac{c}{2\sin\theta} \tag{15}$$

, unless the chord is 0, in which case the radius is 0. The helix angle ϕ is a a function of c and d:

$$\phi = \arctan\frac{c}{d} \tag{16}$$

Sidedness and pitch (s and p) follow directly.

Finally, the vector $\hat{H}$ gives the direction of the axis of the helix, but does not give us a point which fixes it in space. It is most convenient to accept a point B which is a joint and produce the point B_a which is the point on the helix axis closest to B.

To do this, we conceptually construct the midpoint M of $\overrightarrow{BC}$ and utilize the fact that the vector Q from it to its closest point on the axis M_a is perpendicular to the containing both $\overrightarrow{BC}$ and H. Therefore its direction is constructible via cross product, and its length l is computable from the radius and chord. M_a is the midpoint of B_a

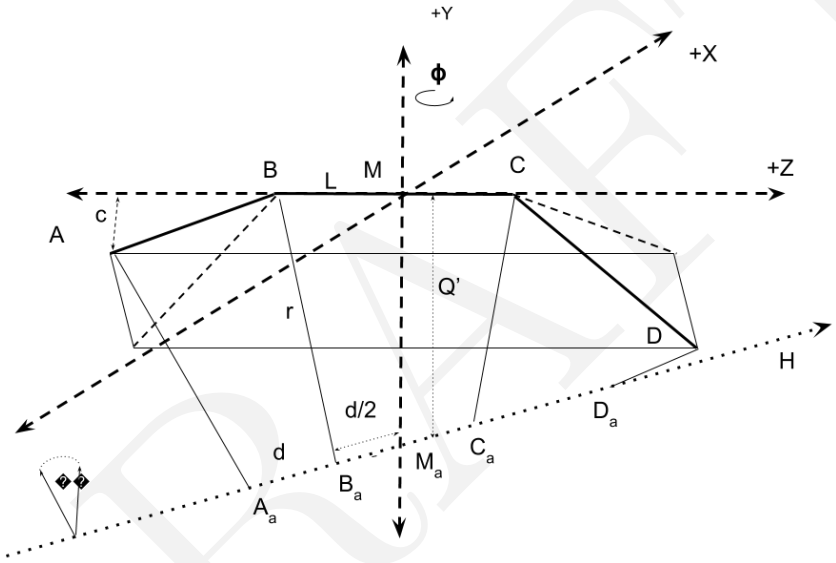

Figure 5: Three Symmetric Members

and C_a, so we can just move back half the travel d along the vector H to get B_a. Figure 5 may be useful in picturing these quantities.

$$C = R(B) \tag{17}$$

$$\overrightarrow{BC} = C - B \tag{18}$$

$$M = \frac{B + C}{2} \tag{19}$$

$$Q = \overrightarrow{BC} \times \hat{H} \tag{20}$$

$$l = \sqrt{r^2 - \frac{c}{2}^2} \tag{21}$$

$$Q' = -\frac{Q}{l} \tag{22}$$

$$B_a = M + Q' - \frac{d}{2}\hat{H} \tag{23}$$

Thus given only the transformation R, the length L, and one joint B, one may compute all of the intrinsic properties (r, θ, d, c, ϕ) of the segmented helix and positioned it in space via H and B_a.

As is common in kinematics[19], there are many ways to represent the same physical or mathematical situation. Four consecutive joint positions also completely determine a segmented helix, as presented below. Because joints can be computed from transformation matrices and transformation matrices from joints, which method of calculation is preferable would be a matter of choice and clarity. We have in fact coded both and used the comparison as automated tests in our software to ensure the correctness of our coding.

A mechanical engineer, robotocist, or computer graphics expert is likely to find the computation from the transformation matrix more natural and convenient. A chemist or crystallographer is more likely to have learned the position of four points and wish to compute from that.

7 *PointAxis*: Computing Segmented Helices from Joints

Kahn[3] has given a method for computing the axis of a helix in the context of chemistry. This method uses the observation that the angle bisectors of the segments on a segmented helix are perpendicular and intersect the axis of the helix. Because the helices may not be perfect and because the measurement of positions may not be perfectly accurate, it is common for chemists to use regression and fitting methods to fit helix parameters to observed positions on the helix. Kahn's method was a prelude to some error-tolerant methods applicable to the realm of organic chemistry. In this paper we are concerned with pure geometry. Also, Kahn was writing in 1989, and we now have more convenient computing tools. We give here a modification of Kahn's algorithm, called *PointAxis*, which relies on our ability, working in the realm of pure geometry, to position the segments on the axes to simplify the derivation and computation.

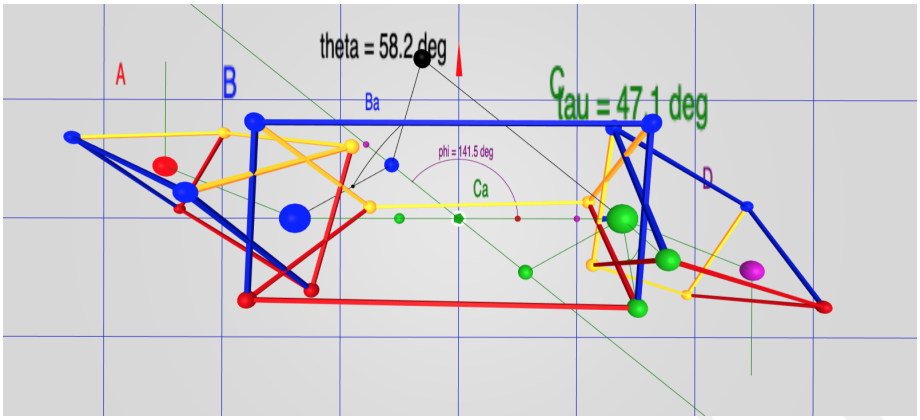

Figure 6: A Balanced Configuration

7.1 A Sketch of the 4-Point Method

Using tools from linear algebra and well-documented algorithms, a sketch of the finding the segmented helix from four consecutive known points A, B, C, D is:

- Compute the bisectors of the angle B_b of $\angle ABC$ and the angle C_b of $\angle BCD$. If the points are collinear, we have a special case.
- Because these angle bisectors point at the axis of the segmented helix, their cross product is a vector in the direction of the axis. If B_b and C_b are parallel or anti-parallel the cross product is not defined and we have special cases.
- Otherwise the vectors B_b and C_b are skew, the algorithm for the closest points on two skew lines provides two points B_a and C_a on these vectors which are the closest points on on those lines and are also points on the axis.
- The distance between B_a and B is the radius, and the distance between B_a and C_a is the travel d along the axis.
- The angle between $\overrightarrow{B - B_a}$ and $\overrightarrow{C - C_a}$ is θ.

7.2 The 4-Point Method

Therefore four consecutive points completely determine at least one segmented helix. We will concern ourselves only with the helix that makes the least rotation between points. The *PointAxis* algorithm with takes four such points (without loss of generality B and C are assumed to be centered on the z-axis, and that a rotation has been performed to balance A and D to that $A_x = -D_x, A_z = -D_z$, and $A_y = D_y$. Thus the input to *PointAxis* in fact has three only three degrees of freedom, which determine the three intrinsic properties r, d, θ which completely define the shape of a segments helix (but not its location in space.) A practitioner may be able to set up the coordinate system such that the four points are in balance; if not, Section 8.1 discuss how to transform them into balance.

Figure 6 shows a downward view of a balanced configuration (though raised above the origin instead of at the origin.) A (the red sphere) is a reflection of D (the purple sphere) across the midpoint. Both A and D are hanging downward. If the structure where hung on a point at the origin, it would be physically balanced. Note it is always possible to achieve this balance, even though a single object itself is not symmetric; in this figure the normal of the B face is not symmetric with C face.

In the derivations below, we rely on certain facts about the segmented helix formed by the stack of objects, the first of which is key:

- Without loss of generality, we may think of any member whose faces and twist generate a non-degenerate helix as being "above" the axis of the helix. We furthermore choose to place the object in this figure so that $B_y = C_y$, that is, that the members are symmetric about the z-axis. A and D are "balanced across the YZ-plane, and $A_x = -D_x$ and $A_y = D_y$.
- Every joint (A, B, C, D) is the same distance r from the axis H of the helix.
- Every member is in the same angular relation ϕ to the axis of the helix.
- Since every member cuts across a cylinder around the axis, the midpoint of every member is the same distance from the axis which is general a little a less than r. In particular the midpoint M whose closest point on the helix axis m is on the y-axis and $\|\overline{Mm}\| < \|\overline{Bb}\|$.
- The points (A_a, B_a, C_a, D_a) on the axis closest to the joints (A, B, C, D) are equidistant about the axis and centered about the y-axis. In particular, $\|\overrightarrow{B - B_a}\| = \|\overrightarrow{C - C_a}\|$.

From the observations that $\|\overrightarrow{B - B_a}\| = \|\overrightarrow{C - C_a}\|$ we concluded that the helix axis is in a plane parallel to the XZ-plane, it intersects the y-axis, but in general is not parallel to the z-axis.

Because the angle bisectors of each joint are in general skew, and intersect the axis perpendicularly, it is clear we can use linear algebra and the algorithm for the closest points on two skew lines to find B_a and B_c.

However, we can take advantage of the fact that a segmented helix has tremendous symmetry, and the angle bisectors are very far from being two generally skew lines. In fact, by taking advantage of the fact that the generating rule for an object chain requires similarity in every joint, we can arrange the objects as in Figure 5.

PointAxis takes a length and a point D known to be in a specific relation to B and C.

We have carefully arranged our axes so that we can compute ϕ, the angle between the helical axis and the z axis. This, in combination with symmetry and the knowledge that the helical axis is in the XZ plane, lets us compute the points on the axis corresponding to the joints directly from ϕ.

This algorithm coded below is simple enough that Mathematica[20] can actually produce symbolic closed-form formula for all computed valued in terms of L, x, y, z, but they are less comprehensible to the human eye than this algorithm, although their existence opens the possibility that, for example, the derivative representing the change in r with a change in D could be calculated.

7.3 Degenerate Cases

Define the angle bisector vectors:

$$B_b = B - (A + C)/2 \tag{24}$$
$$C_b = C - (B + D)/2 \tag{25}$$
$$\tag{26}$$

The fundamental insight that the axis of the helix H can be computed by a cross product of the angle bisector vectors (B_b and C_c) applies only when the angle-bisectors have a non-zero length and when they are not anti-parallel. When the are of zero length, this is the degenerate case of a straight line coinciding with all segments. This occurs only when $A_x = 0 \wedge A_y = 0 \wedge A_z = -3L/2$. In this case:

$$r = 0 \tag{27}$$
$$\theta = \text{undefined} \tag{28}$$
$$d = L \tag{29}$$
$$c = 0 \tag{30}$$
$$\phi = 0 \tag{31}$$
$$H = \begin{bmatrix} 0 \\ 0 \\ L \end{bmatrix} \tag{32}$$
$$B_a = B = \begin{bmatrix} 0 \\ 0 \\ -L/2 \end{bmatrix} \tag{33}$$

H is the direction vector of the helix axis. In this case we do not have enough information to define θ, unless it is through other information. For example, when using the joint-face normal method which specifies the twist τ at the faces, then $\theta = \tau$.

When B_b and C_b are parallel (pointing in opposite directions), the zig-zag degeneracy occurs. Since we are assuming the balance of A and D, this occurs only when

$A_y = 0$. In this case (denoting the x component of the B_a vector as $B_{a[x]}$):

$$B_a = \begin{bmatrix} B_{a[x]} \\ B_{a[y]} \\ B_{a[z]} \end{bmatrix} \tag{34}$$

$$H = C - A \tag{35}$$

$$d = (C - B) \times H \tag{36}$$

$$r = \|B_b\|/2 \tag{37}$$

$$c = 2r \tag{38}$$

$$\phi = \text{atan2}\,(H_z, H_x) - \pi/2 \tag{39}$$

$$c = 0 \tag{40}$$

$$\theta = \pi \tag{41}$$

$$B_{a[x]} = \frac{d\sqrt{1 - (d/L)^2}}{2} \tag{42}$$

$$B_{a[y]} = 0 \tag{43}$$

$$B_{a[z]} = -\frac{d^2}{2L} \tag{44}$$

$$\tag{45}$$

(atan2 is the standard two-argument tangent function employed in software packages.) However, the most general case is simpler, and can be worked out with standard linear algebra operations. In the math below which is a direct analog of our coded solution, we have utilized the tremendous symmetry of the "balance" condition to use mostly scalar operations. There is some hope that this would allow closed-form expressions to be produced, perhaps with the aid of a symbolic computation system such as Mathematica[20]. If completed, this would allow us to give closed-form solution to the intrinsic properties of all the 28 Platonic helices enumerated in Sec 13.

Once H has been calculated, the signed travel along the axis da is the scalar projection of a segment $(C - B)$ onto H. From this ϕ is directly calculatable. ϕ allows a direct calculation of the x, y and z components of the point B_a on the axis pointed to by B_b. r is the distance between Ba and B. c and θ are easily computed from these values.

$$H = \begin{bmatrix} -2B_{b[y]}B_{b[z]} \\ 0 \\ 2B_{b[y]}B_{b[x]} \end{bmatrix} \tag{46}$$

$$d = \frac{LB_{b[x]}}{\sqrt{B_{b[x]}^2 + B_{b[z]}^2}} \tag{47}$$

$$\phi = \text{atan2}\,(H_z, H_x) - \pi/2 \tag{48}$$

$$c = \sqrt{L^2 - d^2} \tag{49}$$

In this approach to calculation, it is easiest for us to compute the axis point B_a corresponding to B and use it to complete our computations.

From trigonometry and utilizing the facts that

$$\phi = \arccos(d/L)$$
$$\sin(\arccos x) = \sqrt{1-x^2}$$

it can be shown that the x and z component of B_a are:

$$B_{a[x]} = \frac{d\sqrt{1-(d/L)^2}}{2} \tag{50}$$
$$B_{a[z]} = -\frac{d^2}{2L} \tag{51}$$

However, this computation exposes another special case: when the helix angle ϕ is $\pi/2$, the segmented helix is a torus-like. In this case the axis point B_a is in fact on the y-axis, and we need only compute $B_{a[y]}$:

$$B_{a[y]} = \frac{LB_{b[y]}}{2B_{b[z]}} \tag{52}$$

When we are not toroidal, we must take $B_{b[x]}$ into account, but it is non-zero, so we can divide by it. By imagining a plane pressed downward from the object axis to the helix axis, we see that $B_{a[y]}$ is proportional to a ration of the angle bisector $B_{b[y]}/B_{b[x]}$ times the $B_{a[x]}$ value:

$$B_{a[y]} = \frac{B_{b[y]}B_{a[x]}}{B_{b[x]}} \tag{53}$$

Having computed all of B_a, the remaining intrinsic properties are easily calculated:

$$r = \|B - B_a\| \tag{54}$$
$$\theta = 2\arcsin\frac{c}{2r} \tag{55}$$
$$\tag{56}$$

7.4 The 4-Point Test

It is useful to have a test if four proposed points really do lie on a segmented helix, to see if they allow valid inputs to *PointAxis* algorithm to be computed via rigid transformation to the z-axis.

Theorem 2 (Segmented Helix Test)**.** *Four arbitrary sequential points A, B, C, D are consecutive joints of a segmented helix if and only if the segments $\overline{AB}, \overline{BC}$, and $\overline{CD}$ are equal length and the scalar projection of $\overrightarrow{CD}$ onto $\overrightarrow{BC}$ is equal to the scalar projection of $\overrightarrow{AB}$ onto $\overrightarrow{BC}$.*

Proof. "If" Case (points on helix imply scalar projections are negations of each other): If A, B, C, D are consecutive joints on a segmented helix, then the angle η between any two consecutive segments is the same. Then:

$$\begin{aligned} \|\overrightarrow{AB}\| &= \|\overrightarrow{CD}\| && \text{Given} \\ \|\overrightarrow{AB}\| \cos\eta &= \|\overrightarrow{CD}\| \cos\eta && \eta \text{ the same for each joint} \\ \overrightarrow{AB} \cdot \hat{\overrightarrow{BC}} &= \overrightarrow{CD} \cdot \hat{\overrightarrow{BC}} && \text{def. of scalar projection} \end{aligned}$$

"only if" Case (equal scalar projections and length imply coincident segmented helix):

If the scalar projections and the lengths are equal, then the cosines of the angles between segments are equal. In the range 0 to π, $\cos\theta = \cos\phi$ implies $\theta = \phi$. Therefore the angles between the segments are equal.

By the previous argument of correctness for the *PointAxis* algorithm, a rigid transformation always exists which balances three such segments. Therefore there always exists a helix axis that is in the xz plane the intersects the y axis and is the same distance from A, B, C and D. This axis is the axis of a segmented helix which rotates each point similarly, provides the same translation along the axis, and maintains the same radius. Hence a segmented helix exists whose joints are A, B, C, and D. □

In a single sentence, if the angles (easily measured by scalar projections) and lengths are the same, they can be brought into our conventional balanced configuration, and form that configuration it is clear there exists a segmented helix that coincides with all joints.

7.5 Comparison

There is one reason one might prefer the transformation matrix method or the point method over the other: with modern computer algebra systems such as Mathematica[20] it might be possible to use these "algorithms" to produce closed-form expressions of closed-form (algebraic) inputs. For example, the Platonic solids all have lengths and face normals which can be specified exactly in closed (thought irrational) form. Thus it might be possible to produce an expression for the radius of one of the Platonic Dodecahelices of unit edge length. We have not undertaken this work.

8 The Joint Face Normal Method

PointAxis takes a point A known to be in a specific, balanced relation to B and C. A chemist might know 4 such points from crystallography, and be able to move them into this symmetric position along the z-axis.

However, we might instead know something of the subunits and how they are conjoined, without actually knowing where points A and D are.

We start with these intrinsic properties of an object, and additionally the rule for how objects are laid face-to-face. That is, knowing the length between two joint points

and a vector normal to the faces of the two joints, we almost have enough to determine the unique stacking of objects. The final piece is that we must know the *twist*. That is, when face A of a second objects is placed on face B of a first object so that they are flush (that is, their normals are in opposite directions), it remains the case that the second object can be rotated about the normals. To define the joining rule, we must attach an *up vector* to each object, or more appropriately since we are dealing with a helix, and *out vector* that points away from the axis. Then a joining rule is "place the second object against the first, joint point coincident to joint point, and twist it so that its up vector differs by τ degrees from the up vector of the first object." In this definition, the up vectors are considered to be measured against the plane containing the two axes meeting in a joint.

Define the *joint plane* to be the plane which contains the two axes meeting in a joint. Define the *joint line* to be the line through the joint perpendicular to the joint plane. Define the *joint angle* to be the angle of the first axis to the second measured about the joint line. The twist τ is the change in the a vector attached to the object rotated about the joint line by the joint angle. That is, take any vector attached to the first object, place it at the joint, rotate it about the joint line via the joint angle. τ is the difference between the angle of this vector measured against the joint plane and the angle of the up vector of the second object measured against the joint plane.

If the objects are macroscopic objects which have faces, this is the same as the rotation of the axis of the second object relative to the first in the plane of the coincident faces. We can identify intrinsic properties:

- An object with two identified faces, labeled B and C. Assume there normalized vectors N_B and N_C from each of these points that is aligned with the axis of the conjoined object attached to that face. This normals might be enforced by the fact that flat faces are joined in the joint plane. However, molecules don't have faces; this conjoining relationship may be enforced some other way.
- The length L of an object, measured from joint point A to joint point B.
- A joint twist τ defining the change in computed out-vector between objects, measured at the joint face.

8.1 Rotating into Balance from Face Normal Vectors

In order to use the *PointAxis* algorithm, we need a way to compute points A and D in balance around the axis BC. A key insight is that Lord's Observation tells us that no matter how lopsided and different the normal vectors N_B and N_C for the joint faces are and no matter what τ we choose, when we conjoin objects their relationship is always the same. After placing BC along the z-axis, there is always an angle ψ which will rotate the points A and D into balance (that is, $(A_x = -D_x) \wedge (A_z = -D_z) \wedge (A_y = D_y)$.

For computer programmers with a graphics library supporting transformation matrices such as THREE.js[21], it is relatively easy to code the math to adjoin objects face-to-face based on the face normals, simulating the physical act of matching flat faces between macroscopic objects.

1. Create the transformation the aligns and centers $\overrightarrow{BC}$ on the z-axis.

2. Create a translation of B to C.
3. Create a rotation of the z-axis to N_B.
4. Create a rotation of of $-N_c$ about N_B.
5. Create a rotation of τ around that axis.

Composing these transformation matrices via multiplication creates a transformation matrix which takes B to C and C to D.

We will assume this as a subroutine called *adjoinPrism* which takes τ (the rotation inside the plane of the joint). A byproduct of balancing the points is the a transformation matrix that takes C into D. Having done this, one can compute the screw axis, and hence all of the segmented helix properties, from either the transformation matrix or the four points. Our code does both and compares the result as a test.

8.2 The Key to Balance

The key insight to finding ψ is to note that we can consider the projections of the B and C face normal vectors projected into the XY plane, and rotate these so that they are balanced around the negative y unit vector. Such a projection into the cross-section of the helix is closely related to the *helical wheel*[22] plot in the study of alpha helices in proteins. Even if the lengths of the projections of the face normals in XY are different, this mechanism works, because by Lord's Observation the points A and D must be symmetric about the segment $\overline{BC}$.

By composing this balancing operation with the face-adjoining transformation matrix, A and D are placed in balance. The screw axis may now be computed from either the four points A, B, C, D or from the transformation matrix created to balance them.

8.3 On the Choice of the Screw Axis Direction

Given only a physical segmented helix without position in space, we may arbitrarily choose the direction for the axis. Changing our decision will make the screw axis point in the negative direction, change the sign of the travel d along the axis, and choose ϕ to be $\pi - \phi$.

As can be seen from interactive play with our software[5], it is entirely possible for the travel along the axis of the helix to be 0–in fact, choosing $\tau \approx 0$ produces toruses, which have no travel along the axis.

We could represent this be making the length of the vector representing the axis be the length of the travel d. However, this would have the drawback than when d is zero we would be unable to determine the axis of revolution of the torus. Although somewhat arbitrary, we have chosen instead to represent the axis as a normalized vector of unit length, and to allow the travel to be negative. This has the benefit that changing τ through (something close to) zero smoothly changes d. However, it creates the problem that as τ approaches (something close to) π from different directions the signs of the axes are different. That is, $\tau \approx \pi$ and $\tau \approx -\pi$ describe exactly the same shape, but in our calculation they will have different signs for the axes. The radius, pitch and absolute value of the travel, which are intrinsic to the shape, will be the same, but the axis vector, ϕ, and the sign of d will be different.

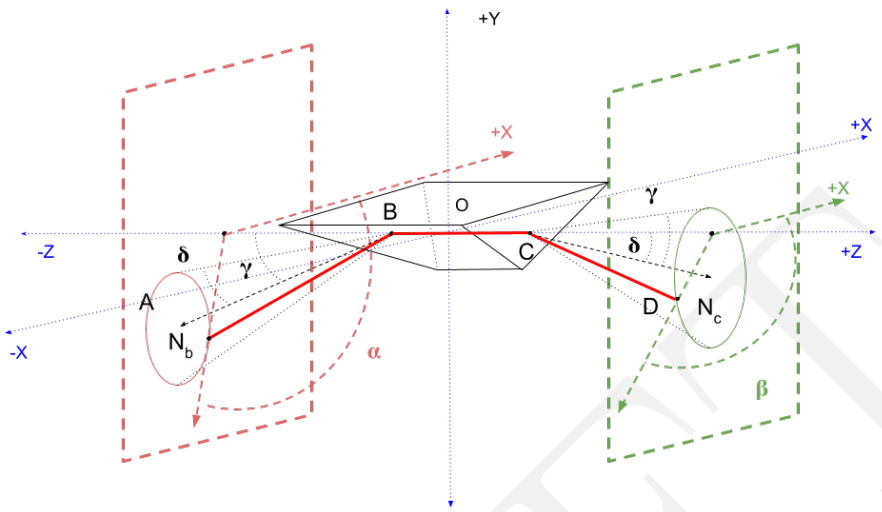

Figure 7: Twist Spectrum Proof Diagram

9 Changing τ Smoothly Changes Tightness

Theorem 3 (Twist Spectrum)**.** *For any choice of non-parallel face normals having non-zero x or y components, changing the twist angle τ through a complete rotation ($0 \leq \tau \leq 2\pi$) smoothly varies the segmented helix between a torus and flat cases.*

Proof. Please see Figure 7, which renders and arbitrary prism in balanced position. The B joint is on the backside of the prism, not visible. As usual, τ is measured against the face. The face normals are labelled N_b and N_c. The are drawn to projection planes orthogonal to the object axis, which is z-axis aligned as per our usual convention. The N_b face normal forms an angle δ with negative z-axis, and the N_c face normal an angle γ with the positive z-axis.

Let the function $\alpha(\tau)$ which is the angle formed by the projection of A and the orign with the X axis in the XY-plane. Let $\beta(\tau)$ be the angle of the D projection. $\alpha(\tau)$ and $\beta(\tau)$ are periodic on τ ranging between 0 and 2π.

Let γ and δ be the angle between the A face-vector and B face-vectors respectively formed with the $\overline{BA}$ vector and $\overline{AB}$ respectively.

If $\gamma \neq \delta$ then one is greater than the other. Without loss of generality, assume $\gamma > \delta$. Then D moves in a cone about the N_c face normal as τ is varied. The angle of the projection of D is β, which varies as τ varies. The projection of both A and D

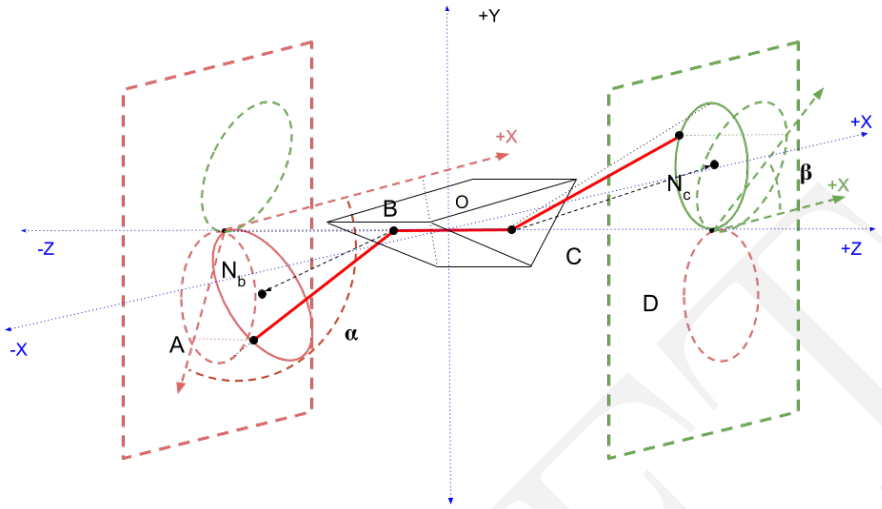

Figure 8: Equal face angle magnitudes

move in circles potentially tilted to the z-axis, thereby forming ellipse-like figures in the projection planes.

By our assumption, because $\gamma > \delta$, the ellipse formed by D as τ changes strictly contains the origin of the projection plane. Therefore at least one of $\beta(\tau)$ has a range containing both 0 and 2π, since the angle swept out by a point on the edge of this figure goes completely around the origin. Without loss of generality, let α have that property.

Both α and β are continuous, by the continuity of physcial mechanisms and the composition of continuous functions.

Note that although the motion need not be proportional, the sign of the motion of $\alpha(\tau)$ is the opposite of the sign of the motion of $\beta(\tau)$ as τ is varied.

Because α varies between 0 and 2π (although β may not), and because β moves in the opposite direction, by the Intermediate Value Theorem, there is a τ where $\alpha(\tau) = \beta(\tau)$. Such a point produces a toroid-like figure.

Since α can be moved in a complete circle (between 0 and 2π), there is always exactly one τ which places α oppsite β (i.e., $\alpha = \pi + \beta$). This is the flat case, which is the maximal extent of the segmented helix.

Now let us consider the case that $\gamma = \delta$, as illustraed in Figure 9.

In this case, the edges of the ellipses formed in the projection plane of both A and D intersect the z-axis, because there is always a τ that rotates the face about the face normal so that they cancel completely. By our proof of segemented helices, this must

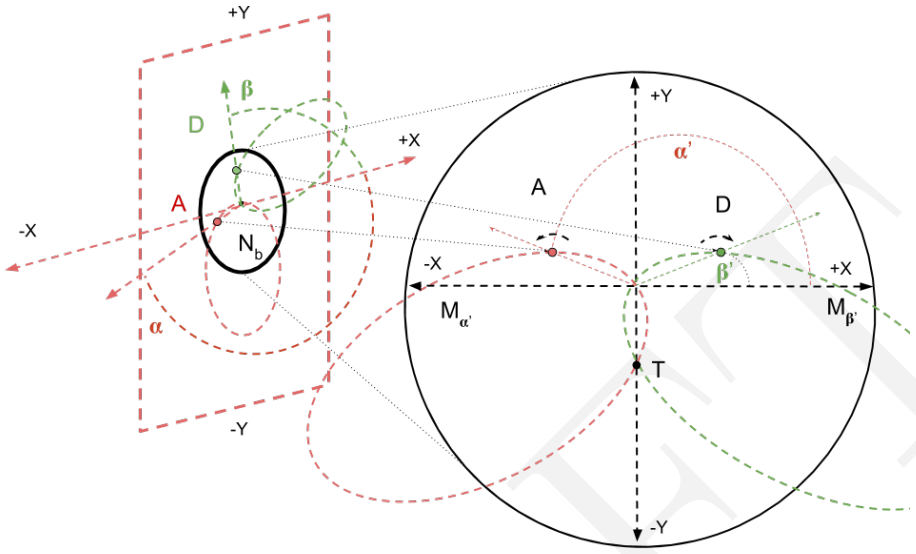

Figure 9: Balanced Projection

occur at the same time on both sides, because the angle of the CD member with BC must equal the angle of the AB member with BC.

Note that the projected ellipses may occur in any relation to each other. Figure **??** illustrates one cirumstance in which the face normal vectors are pointin in approximately opposite directions. If the projections of the face normals are anti-parallel, they will be exactly opposite each other. In this case, the green (D) and red (A) projections will conincide at only one point; this is a straight line or a degenerate torus.

In an unbalanced position, the rate of change or $\alpha(\tau)$ and $\beta(\tau)$ need not be proportional. However, if we always rotate the entire figure into our conventional balanced configuration for any given τ, then the rate of change of α will be exactly opposite β, as illustrated in Figure **??**. Let $\alpha'(\tau)$ and $\beta'(\tau)$ be the angles formed with the negative y-axis in the balanced configuration. By the definition of balance being balanced around the y-axis, $\alpha'(\tau) = -\beta'(\tau)$

This means that the intersection point of the two projected ellipses (which may be very close to the z-axis), will always be reached at exactly time (τ): $\alpha'(\tau) = 0 - \beta'(\tau)$. This intesection point in the balanced configuration is straight down; it is the point at which the projections are in the same plane (and the plane of the z-axis), and at this point the segmented helix is a toroid-like figure. Since there is always such an intersection point and we can move τ through a full rotation, we can always reach such a toroidal point. If the face normals are precisely anti-parallel, this point will occur at the origin, and so will be a straightline which is in a sense a degenerate torus-like

figure, but we do not consider it such.

Similarly, we can always rotate to a point where A and D are pointing opposite each other as measured from the origin of the projection plane, so that $\beta'(\tau) = \alpha'(\tau) + \pm\pi$. This is always the "flat" or maximally extended point. In the balnced convention, this occurs when the projection points are coincident with the x-axis in the projection plane, as shown in Figure **??**. Because in this case $\gamma = \delta$ and A and D points are always (even in the first case of this proof) at equal angles to the z-axis aligned object axis BC, the A and D projection points move at the same speed (with respect to τ), they meet the x-axis at the same τ value.

Thus when the absolute value of the face normals formed with the z-axis are equal, we can smoothly move through a spectrum between the toroid-like figure (zero travel, or $d = 0$), and the position of maximal travel.

□

It would be more useful and elegant to have a formula for the τ that produces a torus as a function of the joint face normals; the authors have not been able to produce such a formula. However, in the calculator page, we numerically provide the τ that produces the minimum tightness (torus-like) and maximum tightness (zig-zag) to the nearest 360-degree, with the labels *Minimum Tightness* τ and *Maximum Tightness* τ.

10 Checks and Explorations

10.1 Qualitative Observations

When the joint face normals are coplanar vectors, then the minimum tightness τ is always 0, and the maximum tightness occurs when $\tau = \pm\pi$. These values deviate from 0 and π roughly in proportion to the non-coplanarity of the normals.

Varying τ smoothly varies the tightness of the coiling of the helix, moving through very linear cases towards a torus, to a torus, to a very linear case on the other side.

In fact it is possible to that there is always a "tightest coil" which does not self-intersect. If we had many objects, we could pack them into a convenient space by computing the τ of the tightest non-self-intersecting coil and stacking them this way. If we had a means to change τ, perhaps via motors in a robot arm, we would have a smoothly telescoping and contracting robot arm or linear actuator. If we had a repated molecular subunit that changed shape in response to an exteranl magnetic or electric field or chemicals in the surrounding environment, we would have a telescoping nanomachine.

10.2 A Brute-force approach to finding Helix Angle from Twist

The calculation methods described in this paper hardly warrant the name "algorithm" when considered from the computational complexity; the are all constant time (for a given fixed precision.) Although involving trigonometric functions, they demand no iteration.

This makes it practical to solve some problems by brute-force iteration. An example already calculated is the twist τ which makes an object product a toroid-like

segmented helix, or on the other hand the τ value that maximizes linear extent and tightness. Future work may allow analytic formulae for τ as a function of tightness to be developed; but in the meantime it is easy enough to simply evaluate objects at many different τ values to find a desired helix angle ϕ, such as 0. One can of course bring standard numerical optimization to bear, because an objective function that depends on the parameters of the segmented helix can be computed in constant time.

11 Implications

One of the implications of having an easily-calculable understanding of the math is that it may be possible to design helices of any radius and pitch by designing periodic (possibly scalene) segments. Combined with slight irregularities, this means that you have a basis of design molecular helices out of "atoms" which correspond to our objects.

This would mean that if you wanted to build a brace of length exactly 3 meters with bars of exactly 1/2 meter you would be able to come as close to this as desired.

A modular robot constructed out of repetitions of the same shape-changing module will always product a helix whose precise shape can be controlled by uniformly changing the shape of all of the modules.

12 Applying to The Boerdijk-Coxeter Tetrahelix

The Boerdijk-Coxeter tetrahelix is a periodic chain of conjoined regular tetrahedra which has been much studied[9, 10, 11, 12] and happens to have irrational measures, making it an ideal test case for our algorithms. Because the face-normals can be calculated and the positions of the elements of the BC helix directly calculated, we can use it to test our algorithms, and in fact these algorithms give the same rotation.

However, it should be cautioned that the helix which Coxeter identified[9] goes through every node of every tetrahedron. Constructing the helix that goes through only "rail" nodes allows irregular tetrahelices to be designed[12]. However, the segmented helices defined in this paper do neither; rather, it is most natural to imagine them moving through the centroid of face of a tetrahedron. This is a segmented helix of very small radius (0.0943) compared to the other two approaches ($\frac{3\sqrt{3}}{10} \approx 0.5196$) which measure the radius to the point of the tetrahedron, but it has the advantage that it is far more general. For example, it is clearly defined if one used truncated tetrahedra. The rotation of a segment matches the BC Helix analytical solution ($\theta = \arctan -3/2 \approx 131.8103$), because a screw transformation does not depend on selecting a point for the radius.

In light of Lord's Observation and the Segmented Helix algorithms, we can now consider the BC Helix and a variety of other segmented helices generated by face-to-face stacking of Platonic solids, examples of called *Platonic segmented helixes*.

Note this also makes clear that in these cases we must also specify the *twist*, even if we insist on perfect face-to-face matching. Thinking of it this way, there are actually three tetrahedral segmented helices, depending on which twist modulo 120° is chosen (keeping the faces matching). In the case of the tetrahedron, this creates the clockwise BC Helix, the anti-clockwise BC Helix, and the not-quite-closed tetrahedral

torus, similar in appearence to but not quite the same as *toriodal polyhedra*[23]. (Five tetrahedra famously lack ≈ 7.356 degrees of being a perfect toriodial polyhedron as can be seen from our sofware which computes $\theta = 70.5288$ for this case, so the gap is $360 - 5 \cdot \theta \approx 7.356$)

In the case of the icosahedron, there are in fact many possibilities, as one need not choose the precisely opposite face as the joining face, and one may choose up to three twists. The "zoo" or Platonic helices can be studied via the calculations described here, and our software makes these interactively selectable (see Section13).

13 The Platonic Helices

In order to demonstrate the utility of the calculations explained in this paper, we have explored periodic chains of the five regular Platonic solids joined face-to-face so that their vertices coincide, which form *Platonic helices.* Such tetrahelices, icosahelices, octahelices and dodechelices have been mentioned in a number of papers[24, 25, 26], but not exhaustively studied in the purely helical form. We propose the name *cubahelix* for the helix made from cubes, as opposed to the equivalent but cumbersome *hexahedronahelix*. Because in some cases Platonic segmented helices may be found in nature or related to structures found in nature[27, 13], it would be convenient to have a table, and images, of all such Platonic segmented helices for reference.

To construct a periodic chain from a Platonic solid, one must decide which faces are joined by the rule. Additionally, one must determine a twist τ as part of the rule, and this twist must be chosen from a small set if the vertices are to coincide. The set of vertex-matching twists differs slightly depending on the face chosen for octahedron, dodacahedron, and icosahedron (but not for the tetrahedron and the cube.) The number of twists in a set will always be equal to the number of sides on a face.

Therefore the number of Platonic helices is in principle a summation of a number of faces times a number of sides, or $4{\cdot}3{+}6{\cdot}4{+}8{\cdot}3{+}12{\cdot}5{+}20{\cdot}3 = 12{+}24{+}24{+}60{+}60 = 180$. However, many of the possibly helices will be indistinguishable if we consider only the shapes produced, as opposed to considering completely labeled or colored faces. Furthermore, every non-toroidal helix will come in clockwise and counter-clockwise version. However, we do not consider rules such as "attach face zero to face zero" which would constitute "doubling back"[24]. The transformation matrix for such a rule would be the identity matrix. It produces an object axis of zero length, a radius of zero, and a travel of zero. It produces perfect self-intersection; that is the entire degenerate helix would appear to be a simply a single Platonic solid.

Using the math in this paper and a computer, it is easy to evaluate all 180 helices, place them in a table, and group them by radius and travel (collapsing chirality). The result is 28 unique shapes. In this number, no provision was made to exclude self-intersection, which does occur, but might not matter to an aerospace engineer building a collapsible space frame of rods and joints. In the language of Elgersma and Wagon[24], not all of the 28 Platonic helices *embedded.*

With those caveats, the helices in Table 1, exemplified by accompanying figures and renderable interactively on our calculator page, thus represents an exhaustive catalog, colloquially called a "zoo", of all Platonic helices.

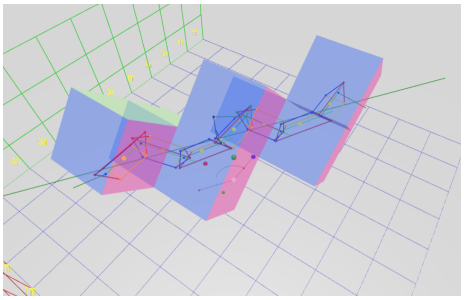

Figure 10: The Blockhelix

Many of the these helices have been previously individually mentioned and even rendered in the literature, though not necessarily fully calculated. In this table, column *C-Face* refers to the face as numbered by the THREE.js software[21], which is somewhat arbitrary. The *# Analogs* column gives the number of Platonic Helices with the same shape, or the enantiomer of it, that is, the same shape in either the clockwise or anticlockwise direction. This list can be expanded completely in our interactive software.

Clearly, for each solid there is a change in twist which keeps the vertices on two joined faces conincident and aligned if they start aligned. This is the $2\pi/n$, where n is the number of sides in a face. The base twist that creates a perfect face-to-face match depends not only on the solid but the face we choose to conjoin to. For each of the Platonic solids, we have just computed this base angle by visual inspection and trial and error. The twist τ of a species of helix in given in the column below.

13.1 Qualitative Descriptions and Interesting Shapes

For fun and to facilitate conversation, we have given all 28 of these Platonic helices nicknames that we find descriptive[1] A few of these are interesting enough to be worthy of particular mention, and comparing them shows the possibility of designing structures using nothing but Platonic solids. The math in this paper works equally well with irregular shapes as well, allowing continuous spectra of designed structures from repeated shapes or molecules.

- "The Blockhelix" (Figure 10) is cubic rectilinear structure in which all angles are right angles; nonetheless a segmented helix hides inside it perhaps not apparent to the human eye at first glance.
- "Pearlshaft" (Figure 11). Conjoining parallel faces always produces a *shaft*. This icosahedron, being relatively round, resembles a string of pearls.
- However, shaft-like helices exist which do not join opposite faces. "The Dodecashaft" (Figure 12) is a remarkably tight non-self-intersecting dodecahelix with

[1]These impressions are likely to be incomprehensible to a non-native speaker of English, or even to somone not born in America in the 1960's. We apologize for this, and hope the value of connoting the shape outweighs this cultural bias.

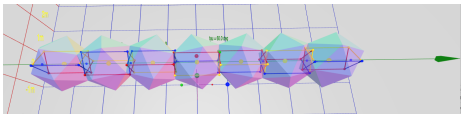

Figure 11: The Pearlshaft

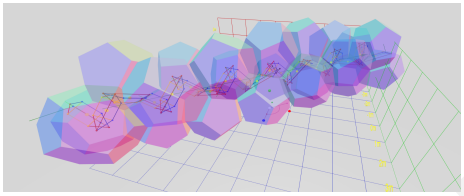

Figure 12: The Dodecashaft
1

very narrow gaps between objects. Such a configuration might be formed by nanofibers under pressure.

- "The Dodecadoubler" (Figure 13) presents the appearance of being a double helix, even though in fact it is a single helix with a simple twist of 72 ° from the Dodecashaft
- "The Dodecacorkscrew" (Figure 14) is a contrasting example of a loose helix, reminiscent of a corkscrew for opening wine bottles.
- The "Quasi-planar" (Figure 15) icoshelix presents a slowly twisting metahelix, so perhaps 10 icosahedron could be said to "lay flat". If this were a molecule or a physical structure made of less-than-perfect rigid members it migt be possible to force it into a pure planar configuration, thus wrapping a cylinder or a plane, studding it with icosahedra.
- "Two Strands" (Figure 16)is similar to the "Dodecadoubler" but even more visually striking. It is reminiscent of a depictions of a DNA double helix.
- "The Wheel" (Figure 17) resembles a modern car tire in proportions. All Platonic solids and indeed all shapes have torus-like configurations. In general they do not "close" perfectly; that is, there is a gap that prevents the final faces from fitting

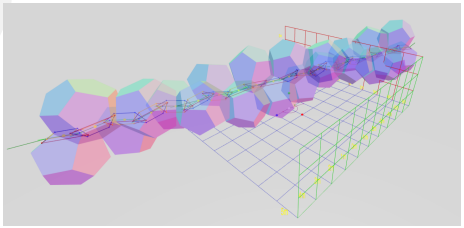

Figure 13: The Dodecadoubler

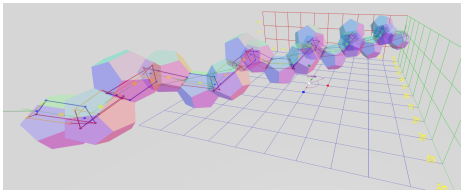

Figure 14: The Dodecacorkscrew

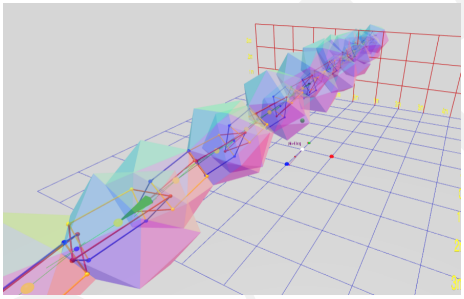

Figure 15: Quasi-planar icosahelix

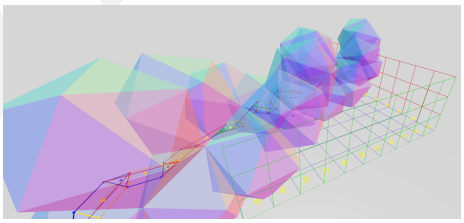

Figure 16: Two Strands

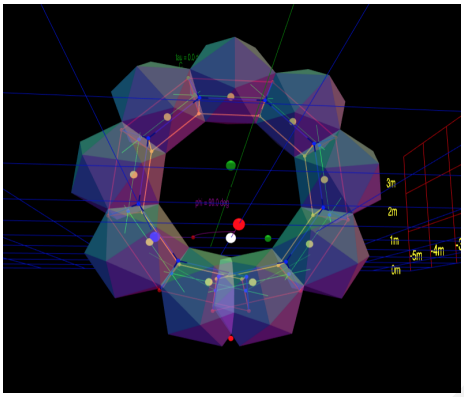

Figure 17: The Wheel

together perfectly. However, one could make tiny adjustment to the repeated shape to close this gap.

14 Future Work

The algorithms and software described herein allow numerical calculation of the intrinsic properties of these Platonic helices, but it would be even better to describe them in with closed-form expressions, as Coxeter did for the Boerdijk-Coxeter tetrahelix. The math and the algorithms are simple enough that if coded in a symbolic algebra system like Mathematica, or with careful work, closed-form expressions could be produced for all the regular Platonic helices. These would be interesting if they happen to be short; we have no reason to believe they will be. The same work could be done for the Archimedean solids. The current work would serve as a useful validation check and intuition-builder for such work.

There may exist a closed-form expression for twist τ which produces a desired helix angle ψ; we have provided only an iterative algorithm for it, which is practical but less elegant.

15 To Do

- Four point proof is shite.
- Add chord, L, etc. to diagram.
- MAJOR BUG: C.z ¡ 0 and B.z ¡ 0 causes mismatch
- Consider application here: https://imbicorg.blogspot.com/p/the-main-objective-of-conference-is-to.html
- Here: http://www.ramsaconference.com/
- Add sidedness to our calculations?

- Modify that so that it truly respects ψ as an input.
- Provide explanation, graphically, if need be, for the computation of B_{ax}, B_{ay}, B_{az} in the general cases.
- Clean up the code. 3 days
- Go through each reference 1 day
- Try to get list of references to the computation of a screw from an arbitrary matrix, and compare and contrast to our code. 1 day
- Need to understand possibility of further simplifying specification of object.
- Need to get this paper, by hook or by crook, and probably cite: Note: An historical review of the theoretical development of rigid body displacements from Rodrigues parameters to the finite twist `https://www.sciencedirect.com/science/article/pii/S0094114X0500087X`
- Improve qualitative section, talk about toruses - 8 hours
- Consider better naming mechanism for faces - 4 hours
- Bibliographic references do not appear to be as detailed as they should be.

16 References that need to be studied or reviewed

Note further that Equations 7 and 8 of this paper[3] give BETTER equations for radius r and the distance d than what I have so far given. Note: I've studied this; I'm not sure there is anything worth doing there.

This is a discussion of segmented coils in a protein structure:
`https://www.sciencedirect.com/science/article/pii/0022283688903701`

A modern helix structure protein paper:
`https://www.sciencedirect.com/science/article/pii/S1476927108000583`

"Simulation of Suspensions of Helical Rigid Fibers" Y Al-Hassan : British Journal of Mathematics and Computer Science (PDF downloaded)

"HELFIT: Helix fitting by a total least squares method" : This needs to be studied closely! `https://www.sciencedirect.com/science/article/pii/S1476927108000418`

QHELIX: A Computational Tool for the Improved Measurement of Inter-Helical Angles in Proteins `https://link.springer.com/article/10.1007/s10930-007-9097-9`

Note:"On the Screw Axes and Other Special Lines Associated With Spatial Displacements of a Rigid Body" `http://manufacturingscience.asmedigitalcollection.asme.org/article.aspx?articleid=1439697`

Note: An historical review of the theoretical development of rigid body displacements from Rodrigues parameters to the finite twist `https://www.sciencedirect.com/science/article/pii/S0094114X0500087X`

17 Acknowledgements

Thanks to Prof. Eric Lord for his direct communication.

The enthusiasm of the participants of the 2018 Public Invention Mathathon intitiated this work.

References

[1] Eric A Lord. Helical structures: the geometry of protein helices and nanotubes. *Structural Chemistry*, 13(3-4):305–314, 2002.

[2] Jens Wittenburg. *Kinematics: theory and applications*. Springer, 2016.

[3] Peter C Kahn. Defining the axis of a helix. *Computers & chemistry*, 13(3):185–189, 1989.

[4] Robert L. Read. Segmented helix javascript code. `https://github.com/PubInv/segmented-helixes/blob/master/js/segment_helix_math.js`, 2019.

[5] Robert L. Read. Segmented helix interactive 3d calculator. `https://pubinv.github.io/segmented-helixes/index.html`, 2019.

[6] Robert L. Read. The story of a public, cooperative mathathon, December 2019. [Online; posted 12-December-2019].

[7] Nasser M. Abbasi. Review of the geomety of screw axes, June 2015.

[8] Wikipedia contributors. Screw axis — Wikipedia, the free encyclopedia, 2019. [Online; accessed 6-June-2019].

[9] HSM Coxeter et al. The simplicial helix and the equation tan(n θ) = n tan(θ). *Canad. Math. Bull*, 28(4):385–393, 1985.

[10] Garrett Sadler, Fang Fang, Julio Kovacs, and Klee Irwin. Periodic modification of the Boerdijk-Coxeter helix (tetrahelix). *arXiv preprint arXiv:1302.1174*, 2013.

[11] R.B. Fuller and E.J. Applewhite. *Synergetics: explorations in the geometry of thinking*. Macmillan, 1982.

[12] Robert Read. Transforming optimal tetrahelices between the boerdijk-coxeter helix and a planar-faced tetrahelix. *Journal of Mechanisms and Robotics*, June 2018.

[13] Peter Pearce. *Structure in Nature is a Strategy for Design*. MIT press, 1990.

[14] Wikipedia contributors. Helix angle — Wikipedia, the free encyclopedia, 2019. [Online; accessed 17-June-2019].

[15] Lizhi Gu, Peng Lei, and Qi Hong. Research on discrete mathematical model of special helical surface. In *Green Communications and Networks*, pages 793–800. Springer, 2012.

[16] Wikipedia contributors. Chasles' theorem (kinematics) — Wikipedia, the free encyclopedia, 2018. [Online; accessed 19-June-2019].

[17] Wikipedia contributors. Rigid transformation — Wikipedia, the free encyclopedia, 2019. [Online; accessed 21-June-2019].

[18] Wikipedia contributors. Rotation matrix — Wikipedia, the free encyclopedia, 2019. [Online; accessed 21-June-2019].

[19] Janez Funda and Richard P Paul. A computational analysis of screw transformations in robotics. *IEEE Transactions on Robotics and Automation*, 6(3):348–356, 1990.

[20] Wolfram Research, Inc. Mathematica, Version 12.0. Champaign, IL, 2019.

[21] Jos Dirksen. *Learning Three. js: the JavaScript 3D library for WebGL*. Packt Publishing Ltd, 2013.

[22] Wikipedia contributors. Helical wheel — Wikipedia, the free encyclopedia, 2018. [Online; accessed 13-July-2019].

[23] Wikipedia contributors. Toroidal polyhedron — Wikipedia, the free encyclopedia, 2018. [Online; accessed 13-July-2019].

[24] Michael Elgersma and Stan Wagon. The quadrahelix: A nearly perfect loop of tetrahedra. *arXiv preprint arXiv:1610.00280*, 2016.

[25] Hassan Babiker and Stanisław Janeczko. *Combinatorial cycles of tetrahedral chains*. IM PAN, 2012.

[26] EA Lord and S Ranganathan. Sphere packing, helices and the polytope {3, 3, 5}. *The European Physical Journal D-Atomic, Molecular, Optical and Plasma Physics*, 15(3):335–343, 2001.

[27] EA Lord and S Ranganathan. The γ-brass structure and the boerdijk–coxeter helix. *Journal of non-crystalline solids*, 334:121–125, 2004.

Table 1: The Platonic Helices

Name	Solid	# Analogs	C-Face #	τ	radius	θ	d	ϕ
Tetrahelix	Tet	6	1	-120	0.094	131.810	-0.516	161.565
Tetratorus	Tet	3	1	0	0.471	70.529	0.000	90.000
Boxbeam	Cub	4	1	-180	0.000	0.000	1.000	0.000
Staircase	Cub	4	2	-180	0.000	0.000	0.707	0.000
Blockhelix	Cub	8	2	-90	0.236	120.000	-0.577	144.736
Cubatorus	Cub	4	2	0	0.500	90.000	0.000	90.000
Octabeam	Oct	3	5	-60	0.000	0.000	1.155	0.000
Octaspikey	Oct	6	1	-120	0.148	146.443	-0.603	154.761
Octamedium	Oct	6	2	-120	0.163	131.810	-0.894	161.565
Octagear	Oct	3	1	0	0.408	109.471	0.000	90.000
Treestar	Oct	3	2	0	0.816	70.529	0.000	90.000
Dodecabeam	Dod	5	8	-108	0.000	0.000	1.589	0.000
Dodecadoubler	Dod	10	1	-144	0.113	161.301	-0.805	164.550
The Alternater	Dod	10	2	-144	0.118	149.520	-1.333	170.306
Dodecashaft	Dod	10	1	-72	0.351	129.657	-0.543	130.501
Dodecagear	Dod	5	1	0	0.491	116.565	0.000	90.000
Dodecacorkscrew	Dod	10	2	-72	0.546	93.026	-1.095	144.110
Dodecadonut	Dod	5	2	0	1.286	63.435	0.000	90.000
Pearlshaft	Ico	3	13	-60	0.000	0.000	1.589	0.000
Quasi-planar	Ico	6	8	165	0.049	167.764	1.294	4.347
Two Strands	Ico	6	1	120	0.137	159.446	0.499	28.340
Slow Twist	Ico	6	12	120	0.169	124.309	1.454	11.641
Rock Candy	Ico	12	2	120	0.204	146.443	0.830	25.239
Icosa Tree Star	Ico	3	1	0	0.304	138.190	0.000	90.000
Icosacorkscrew	Ico	6	8	-75	0.512	99.253	-1.037	143.042
Planar point cluster	Ico	6	2	0	0.562	109.471	0.000	90.000
Big Icosacorkscrew	Ico	6	8	45	0.803	82.064	0.756	54.343
The Wheel	Ico	3	12	0	2.080	41.810	0.000	90.000